PCCP

Pretransitional behavior of viscoelastic parameters at the uniaxial to twist-bend nematic phase transition in flexible n-mers

SCHOLARONE™
Manuscripts

Journal Name

ARTICLE TYPE

Pretransitional behavior of viscoelastic parameters at the nematic to twist-bend nematic phase transition in flexible n-mers[†]

Zeinab Parsouzi,[a‡] Greta Babakhanova,[b,c‡] Mojtaba Rajabi,[a] Rony Saha,[a] Prabesh Gyawali,[a] Taras Turiv,[b,c] Hao Wang,[b,c] Alan R. Baldwin,[a] Chris Welch,[d] Georg H. Mehl,[*d ||] J. T. Gleeson,[a] Antal Jakli,[a,b,c] Oleg D. Lavrentovich,[a,b,c §] and Samuel Sprunt[*a¶]

We report dynamic light scattering measurements of the orientational (Frank) elastic constants and associated viscosities among a homologous series of liquid crystalline dimer, trimer, and tetramer exhibiting a uniaxial nematic (N) to twist-bend nematic (N_{TB}) phase transition. The elastic constants for director splay (K_{11}), twist (K_{22}) and bend (K_{33}) exhibit the relations $K_{11} > K_{22} > K_{33}$ and $K_{11}/K_{22} > 2$ over the bulk of the N phase. Their behavior near the N–N_{TB} transition shows a dependency on the parity of the number (n) of the rigid mesomorphic units in the flexible n-mers. Namely, the bend constant K_{33} in the dimer and tetramer turns upward and starts increasing close to the transition, following a monotonic decrease through most of the N phase. In contrast, K_{33} for the trimer flattens off just above the transition and shows no pretransitional enhancement. The twist constant K_{22} increases pretransitionally in both even and odd n-mers, but more weakly so in the trimer, while K_{11} increases steadily on cooling without evidence of pretransitional behavior in any n-mer. The viscosities associated with pure splay, twist-dominated twist-bend, and pure bend fluctuations in the N phase are comparable in magnitude to those of rod-like monomers. All three viscosities increase with decreasing temperature, but the bend viscosity in particular grows sharply near the N-–N_{TB} transition. The N–N_{TB} pretransitional behavior is shown to be in qualitative agreement with the predictions of a coarse-grained theory, which models the N_{TB} phase as a "pseudo-layered" structure with the symmetry (but not the mass density wave) of a smectic-A^* phase.

1 Introduction

The twist-bend nematic (N_{TB}) phase is the most recently discovered, as well as one of the most intriguing, manifestations of molecular orientational order in soft matter. Meyer[1] originally conjectured the existence of a stable combination of twist and bend distortions in the nematic state of achiral mesogens with

[a] Department of Physics, Kent State University, Kent, OH 44242 USA.

[b] Advanced Materials and Liquid Crystal Institute, Kent State University, Kent, OH 44242 USA.

[c] Chemical Physics Interdisciplinary Program, Kent State University, Kent, OH 44242 USA.

[d] Department of Chemistry, University of Hull, Hull HU6 7RX UK.

† Electronic Supplementary Information (ESI) available: [details of any supplementary information available should be included here]. See DOI: 10.1039/b000000x/

‡ These authors contributed equally to this work.

|| Email: g.h.mehl@hull.ac.uk

§ Email: olavrent@kent.edu

¶ Email: ssprunt@kent.edu

a bent conformation. Subsequently, Dozov[2] proposed a Landau theory to describe a transition from the normal uniaxial nematic (N) to the N_{TB} state that is driven by negative bend elasticity. Additional theoretical[3,4] and molecular simulation[5] studies have also addressed the question of unconventional nematic phases formed by bent mesogens.

Experimentally, the twist-bend structure was first established[6–14] in liquid crystal dimers consisting of two rod-like mesogenic arms connected by a flexible spacer having an odd number of methylene groups. The odd-membered linkage is considered to impose an average conformational bend, which reduces the elastic energy of bend distortions of the nematic director. Simultaneous twist of the director then enables the bend to propagate through space without high energy singularities. The N_{TB} structure typically develops from the uniaxial N phase and not directly from the isotropic state.

The initial experimental results spurred further theoretical de-

velopment[15–19], and the combination of efforts have elucidated several remarkable properties of the N_{TB} phase:

First, even though the constituent molecules are achiral, the N_{TB} phase has a spontaneously chiral structure[9,20,21]. The molecules are of an overall bent shape and a twisted molecular conformation is favored in the N_{TB} phase, as measured by NMR techniques[22]; this results in an overall heliconical packing, with the molecular long axis inclined at an average angle β with respect to the direction around which it precesses (i.e., with respect to the average optical axis, or uniaxial nematic director). The heliconical rotation can be either left- or right- handed, and domains of each coexist.

A second remarkable feature is the surprisingly small periodicity (or pitch p_0) of the heliconical rotation. In the majority of materials investigated thus far, p_0 is only a few times the molecular length (~ 10 nm), far less than the period of chiral modulation observed in cholesteric or ferroelectric liquid crystals. Special experimental methods, including freeze fracture transmission electron microscopy (FFTEM)[7,8] and resonant x-ray scattering (RXS)[23–26], are required to determine the nanoscale pitch of the N_{TB} phase.

Third, and as a result of the extremely short pitch, the behavior of the N_{TB} phase on optical and similar mesoscopic scales can be understood by invoking a "pseudo-layered" structure, with the effective "layer" spacing being equal to p_0. The pseudo-layers have the symmetry of a smectic-A (or, more precisely, a smectic-A*) phase, although they differ from "true" layers in that no mass density wave is observed. The N_{TB} phase should therefore exhibit a smectic-like spectrum of fluctuation modes as well as other interesting properties such as an electroclinic effect, and indeed these have been confirmed by electro-optical[9] and light scattering[27,28] measurements.

Characteristic textural defects in the pseudo-layer structure, and the behavior of orientational elastic constants in the higher temperature N phase, enable one to identify the N_{TB} phase through conventional optical methods. On cooling below the N—N_{TB} transition ($T = T_{NTB}$), shrinkage in the pseudo-layer spacing (decreasing p_0) causes the pseudo-layer planes (planes of constant heliconical phase) to buckle, producing a striped optical texture and the appearance, at lower temperature or near the surfaces of untreated sample cells, of smectic-A-like focal conic defects.[7,19,29,30] As $T \to T_{NTB}$ from above, the bend elastic constant decreases; if the "bare" splay to twist elastic constant ratio exceeds 2, a twist-bend modulation is favored at lower temperature[2].

To date, liquid crystal dimers have been the primary focus for experimental studies of twist-bend and other possible nanomodulated nematic states, but there is growing interest in investigating how these phenomena extend to higher n-mers with odd parity flexible linkages[31–34]. Indeed, the N_{TB} phase has recently been identified in flexible, hybrid bent-core[35] and straight-core[36] trimers and also in a tetramer[37]. Interestingly, it appears that the behavior of important parameters describing the twist-bend modulation may vary qualitatively with the number of monomeric units. Carbon-edge RXS and FFTEM measurements[36] reveal that the nanoscale pitch p_0 in the N_{TB} phase of a trimer is tempera-

ture independent, in contrast to the behavior in the homologous dimer, and is surprisingly shorter than in the dimer. This result poses the question of whether the nature or process of twist-bend ordering may vary with the number of mesogenic units n, and how this difference might be detected in the behavior of macroscopic as well as microscopic properties. A particularly intriguing question is whether the effects of N_{TB} ordering on the macroscopic properties may differ for even and odd n, as the aforementioned RXS results indicate for the microscopic parameter p_0.

In this paper, we present a comparative study of the orientational (Frank) elastic constants and associated orientational viscosities in the uniaxial N phase of a homologous dimer, trimer, and tetramer that contain identical, odd parity linkages between the mesogenic units and exhibit a N—N_{TB} transition. In addition to measuring these parameters as a function of temperature, we report differences in the pretransitional behavior of a certain subset of them. The most notable difference occurs in the bend elastic constant K_{33}. After softening on cooling through most of the uniaxial N phase, K_{33} abruptly starts increasing in the dimer and tetramer close to the transition; on the other hand, there is no indication of an increase in K_{33} in the trimer. This observation suggests an odd-even effect of a new type in flexible n-mers. The associated bend viscosity η_{bend} exhibits a pretransitional enhancement in each of the n-mers, as does the twist elastic constant K_{22}. On the other hand, the splay constant K_{11}, and the corresponding viscosity η_{splay}, show no enhancement. We discuss these results in terms of a coarse-grained theory of the N–N_{TB} transition, which treats the N_{TB} phase as a "pseudo-layered" structure with symmetry equivalent to a smectic-A* phase, and which maps the coefficients in the associated coarse-grained Landau-deGennes free energy onto those appearing in various "local" models that explicitly account for the local heliconical structure. Our light scattering experiments probe length scales ~ 50 times longer than the typical N_{TB} pitch, so the coarse-grained theory provides an appropriate framework for analyzing them.

2 Experimental details

The chemical structures and certain details on the synthesis of the studied oligomers – the dimer 1,5-Bis(2',3'-difluoro-4"-pentyl-[1,1':4',1"-terphenyl]-4-yl)nonane (DTC5C9, previously reported in refs[7,38]), its homologous trimer and tetramer, as well as the monomer 2', 3'-difluoro-4,4"-dipentyl-p-terphenyl (MCT5) – are given in Fig. 1. The synthetic route to the trimer **6** and tetramer **7**, starting from literature reported compounds **1** and **2**, involves four steps. Full synthetic details including spectroscopic characterization and analysis are given in the ESI. Starting from compounds **1** and **2**, a Pd(PPh$_3$)$_4$ catalysed cross coupling (Suzuki Miyaura) furnished intermediate **3** in 79% isolated yield. This compound exhibits two nematic mesophases on heating, N_{TB} ($43 - 57°C$) and N ($57 - 74°C$). A subsequent Suzuki Miyaura coupling reaction with 1,2-difluorophenyl-3-boronic acid resulted in the intermediate **4** which also shows a N_{TB} phase, but this is now seen on cooling only. A low temperature lithiation of compound **4** with ^{n}BuLi at $-78°C$, and subsequent reaction with boron trimethylester gave **5** in a yield of 81%. A reaction of **5** with **3** under Suzuki conditions resulted in the trimer
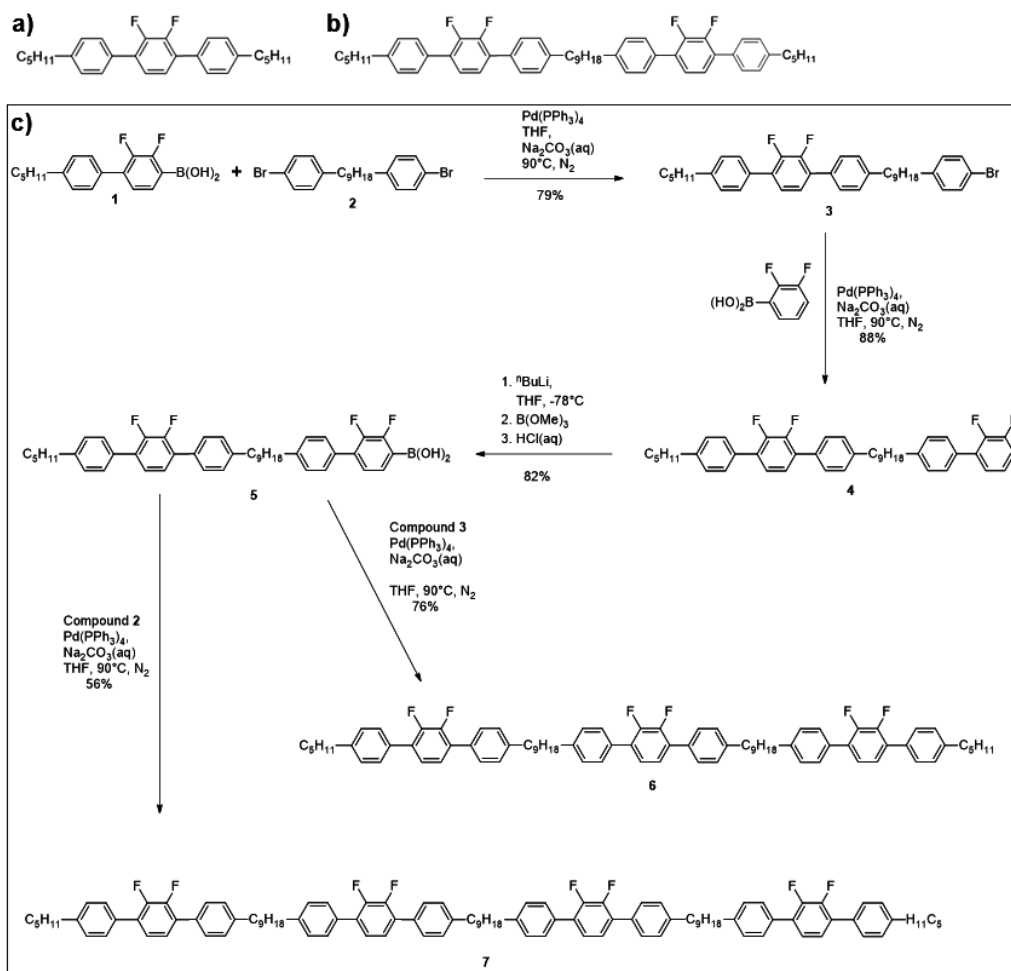
Fig. 1 a) and b): Molecular structures of MCT5 monomer and DTC5C9 dimer. c): Synthetic scheme for the homologous trimer **6** and tetramer **7**.
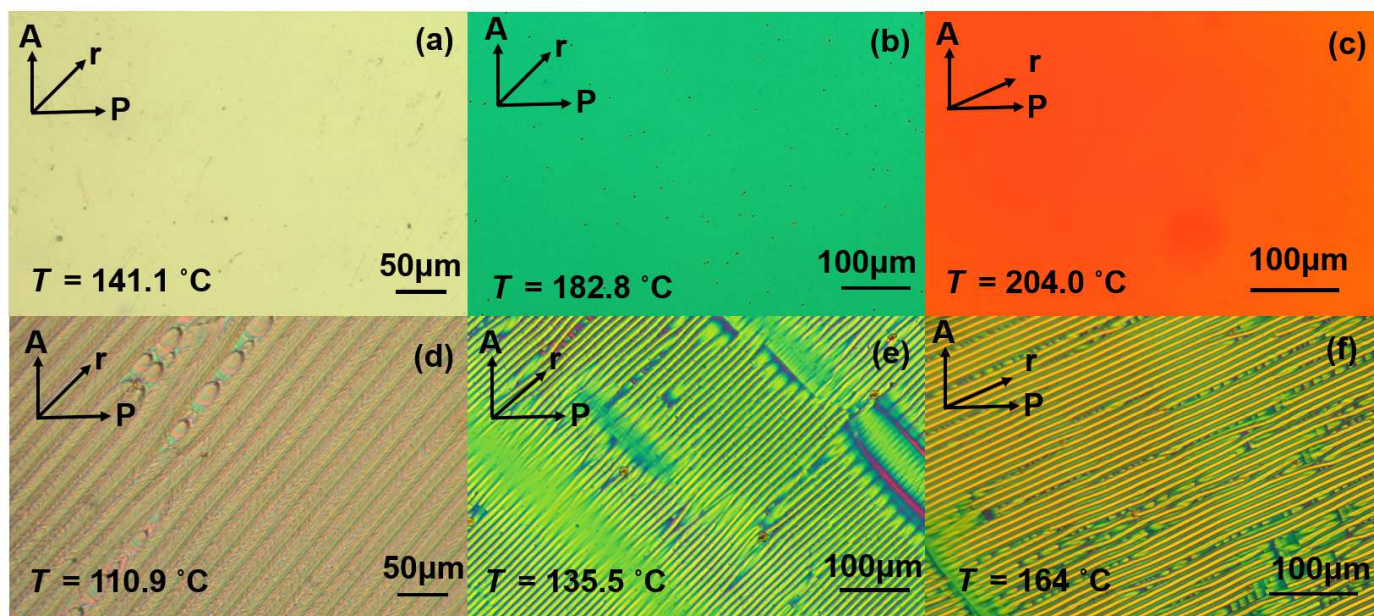

Fig. 2 Polarizing optical microscopy textures of the dimer, trimer, and tetramer: a), b), and c), respectively, the aligned uniaxial nematic phase, and d), e), and f), respectively, the nematic twist-bend phase, exhibiting characteristic stripes parallel to the orientation of the average director.

6 in a yield of 76%. After crystallization from a mixture of dichloromethane/acetone and using the same conditions, compounds **5** and **2** were reacted together in a 1:2 molar ratio to give the tetramer **7** in 56% yield. The phase properties of **3** and **4** are interesting, but we shall not discuss them further here.

Thermal characterization of the dimer, trimer, and tetramer was performed by consecutive differential scanning calorimetry experiments using a Mettler Toledo DSC822e instrument; for details and results, see the ESI.

We conducted polarizing optical microscopy (POM) and dynamic light scattering (DLS) studies on samples of these n-mers contained in optical cells, which were treated for homogeneous planar alignment of the nematic director. Prior to filling each cell, we determined the gap between the substrates to an accuracy of ± 0.1 μm, using a UV/VIS Spectrometer (Perkin Elmer, Lambda 18). The sample thicknesses ranged from 4.8 to 17.7 μm. For temperature-dependent measurements, the sample cells were placed in an Instec HCS402 hot stage (regulated to a precision of $0.01°$C). The I–N and N–N_{TB} transitions, determined by POM in cooling, were, respectively, 162 and 124°C (dimer), 192 and 145°C (trimer), and 205 and 168°C (tetramer).

In our DLS measurements, we used two laser light sources, an optically pumped semiconductor laser (Coherent Genesis model MX-SLM) operating at 532 nm and a HeNe laser (Spectra-Physics, model 127) operating at 633 nm. The scattered light intensity is proportional to the amplitude of nematic director fluctuation modes, which is controlled by the magnitude of the K_{ii} and by the wavevector of the mode selected out through the choice of scattering geometry.

Because absolute measurements of the scattered intensity are difficult, DLS is more often used to determine ratios of the elastic constants than to measure absolute values. For our study, we prepared a reference sample of the thermotropic nematic 4-n-octyloxy-4'-cyanobiphenyl (8OCB), for which accurate, published values of the individual K_{ii} are available[39–41]. A cell containing 8OCB was situated in the same plane in the hot stage as the cells filled with the test n-mers. Both the reference and test cells were assembled from identical sets of substrates treated with identical alignment layers. The reference cell was illuminated by the same incident laser beam (~ 4 mW power focused to a waist diameter of ~ 50 μm) as the test cells, and scattering was collected and processed with the same combination of pinhole, imaging optics, photomultiplier detectors, and photon counting electronics. The optical textures of both test and reference samples were monitored at all times to ensure that only well-aligned, defect-free volumes were illuminated.

As described in ref[42], measurements of the scattered intensity from pure bend fluctuations were made on the reference and test samples for several temperatures, $T_{NI} - T$, relative to nematic-isotropic transition at T_{NI}. Together with accurate determination of the sample thicknesses, measured or published values of the dielectric anisotropy at the various $T_{NI} - T$ and fixed incident light wavelength, and using the calculated expression for the scattered intensity, we calibrated K_{33} for the test samples against the literature values for 8OCB. The calibrated K_{33} were then combined with light scattering measurements of the ratios K_{11}/K_{33}

and K_{22}/K_{33} to obtain values of K_{11} and K_{22}. Further details of the scattering geometries used to make these measurements are provided in the ESI.

To determine the orientational viscosities, we recorded the time correlation function of the scattered light intensity in each scattering geometry. Fitting these data to an exponential decay in time yields the relaxation rates Γ for the director fluctuations probed. In particular for splay and bend scattering (isolated using the so-called "magic" scattering angle – see the ESI), we have $\Gamma_1 = K_{11}q_\perp^2/\eta_{splay}$ and $\Gamma_3 = K_{33}q_z^2/\eta_{bend}$, where η_{splay} and η_{bend} are the effective orientational viscosities for splay and bend fluctuations, and $q_\perp$ (q_z) is the component of the scattering vector perpendicular (parallel) to the nematic director $\hat{n}$. As explained in the ESI, our measurements of twist fluctuations contained a small component of bend. In this case the relaxation rate is $\Gamma_2 = K_{22}q_\perp^2/\eta_{twist-bend}$, where $\eta_{twist-bend}$ is the viscosity for relaxation of the twist-bend mode at the small scattering angle $\theta = 2°$ used to study predominantly (but not purely) twist fluctuations. Combining our results for K_{ii} and Γ_i, we then determined η_{splay}, $\eta_{twist-bend}$, and η_{bend} as functions of T.

3 Results

Differential scanning calorimetry (DSC) data for the transition enthalpies and entropies of the n-mers are tabulated in the ESI; both thermodynamic quantities increase at the N–N_{TB} and I–N transitions with increasing n, but have magnitudes similar to those observed in small molecule nematic LCs. For each n-mer, the enthalpy and entropy at the I–N transition are larger than measured at the N–N_{TB} transition. These results suggest a weak first-order N–N_{TB} transition in the studied n-mers – weaker for lower n – although confirmation of the order of the transition by thermal analysis alone normally requires measurement of the specific heat by ac or adiabatic calorimetry or by modulated DSC (MDSC) methods[43,44]. So far, MDSC data are only available for the dimer, where they do indeed indicate a weak first-order transition[38].

As Fig. 2 shows, the aligned uniaxial N phase of each n-mer exhibits a uniform optical texture. At lower temperatures, optical stripes, parallel to the average director and characteristic of pseudo-layer formation in the N_{TB} phase, nucleate and grow. The N to N_{TB} transition is signaled by a well-defined propagating front observed in cooling by POM at a temperature slightly above the point where the stripe pattern develops; such a clearly delineated front is consistent with a first-order phase transition[45]. While direct measurements of the nanoscale structure are not yet available for the pure n-mers, previous FFTEM results[7] on mixtures of the DTC5C9 dimer with its monomeric building block (MCT5) clearly reveal the "pseudo-layers", as well as periodic textural arches (asymmetric Bouligand arches), that confirm a N_{TB} structure. Additionally, Se-edge RXS has verified a nanoscale orientational modulation, characteristic of the N_{TB} phase, in a homologous dimer with Se atoms substituted on opposing ends of the monomeric cores[24].

Fig. 3 presents our DLS measurements of the orientational elasticities K_{11}, K_{22}, and K_{33} for the dimer, trimer and tetramer. In order to display the temperature dependence over a uniform range that is convenient for comparing pretransitional behavior among
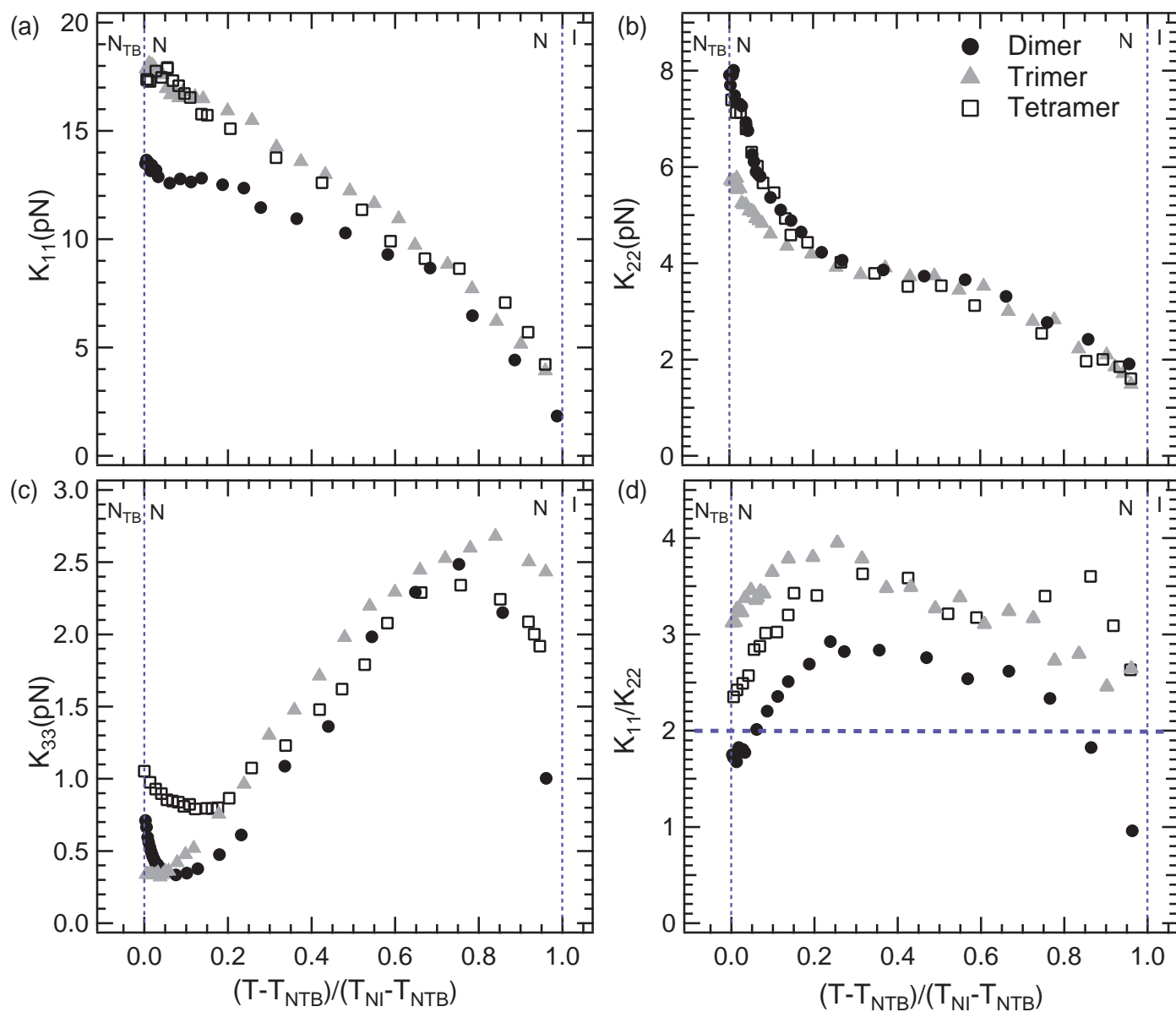
Fig. 3 Reduced temperature dependences of the nematic elastic constants. (a) – (c): Splay (K_{11}), twist (K_{22}), and bend (K_{33}) constants for the dimer, trimer, and tetramer; (d): The ratio K_{11}/K_{22} with the theoretical threshold value for a N_{TB} phase indicated by a horizontal dashed line.
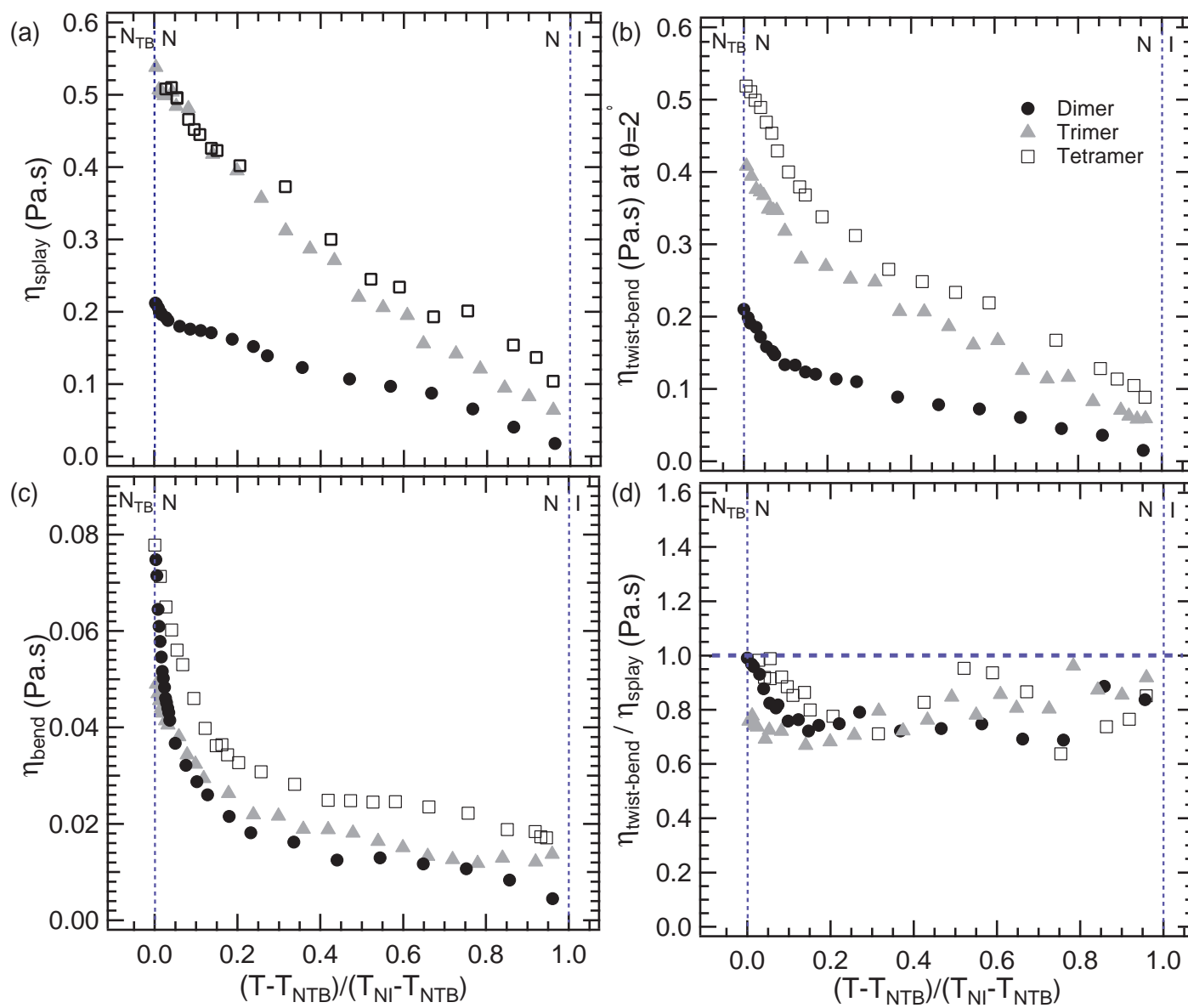
Fig. 4 Reduced temperature dependences of the nematic orientational viscosities in the studied n-mers. (a) − (c): η_{splay}, $\eta_{twist-bend}$, and η_{bend}; (d): The ratio $\eta_{twist-bend}/\eta_{splay}$.

Fig. 5 Elastic constants (a) and viscosities (b) as a function of reduced temperature in the N phase of the monomer MCT5. T_{NCr} is the temperature of the nematic to crystal transition.

the full nematic range, as expected theoretically for n-mers that exhibit the NTB phase[2]. The ratio skews slightly downward close to the both the N—N_{TB} and N—I transitions. The dimer shows similar behavior, although the ratio drops below 2 close to the transitions. The reason for the downward trend as $T \to T_{NTB}$ is the pretransitional increase of K_{22} relative to K_{11} (Fig. 3(b) vs 3(a)). As we will discuss in the next section, this increase results from renormalization of the "bare" K_{22} due to fluctuating pseudo-layer domains. Approaching T_{NI}, differences in the detailed dependences of K_{11} and K_{22} on nematic order parameter S may produce a downward shift in their ratio as $T \to T_{NI}$. The criterion K_{11}/K_{22} for a twist-bend modulation is based on "bare" values of K_{11} and K_{22} — i.e., values corresponding to well-developed nematic order but no significant impact of pretransitional N_{TB} fluctuations. In this region of Fig. 3(d), the measured K_{11}/K_{22} clearly exceeds 2 for all three n-mers.

Fig. 4 displays the temperature dependence of the orientational viscosities η_{splay}, $\eta_{twist-bend}$, and η_{bend} in the N phase. With decreasing T, the viscosities grow monotonically, with η_{bend} showing the most pronounced pretransitional increase as $T \to T_{NTB}$. This increase is more marked in the dimer and tetramer than in the trimer. We see that η_{bend} is much smaller than the other two viscosities, as is normally found in rod-shaped monomeric nematics.

According to standard nematohydrodynamics[46], we expect the pure twist viscosity to exceed η_{splay}, although they usually have comparable magnitudes in typical rod-like nematics. Our measurement of $\eta_{twist-bend}$ is systematically lower than η_{splay} (Fig. 4(d)). However, $\eta_{twist-bend}$ contains a $\vec{q}$-dependent mixture of the director twist viscosity and other fundamental viscosities, including the Miesowicz viscosities that are associated with the coupling of shear flow to the director motion. If the Miesowicz viscosities are sufficiently anisotropic, a small contribution of bend to the scattering from the twist-bend mode (small component of q_z in the scattering vector) could significantly depress $\eta_{twist-bend}$ toward the much lower value of η_{bend}. Thus, our experimental result $\eta_{twist-bend} < \eta_{bend}$ in Fig. 4(d) is not unexpected and probably does not indicate a departure from the normal behavior in uniaxial nematics.

For completeness, we present in Fig. 5 DLS data for the viscoelastic parameters in the N phase of the monomer MCT5 (Fig. 1(a)), plotted versus reduced temperature $(T - T_{NCr})/(T_{NI} - T_{NCr})$ where T_{NCr} is the nematic to crystal transition temperature. Both the elastic constant and viscosity data exhibit conventional behavior in the N phase, with $K_{33} \gtrsim K_{11} > K_{22}$ and $\eta_{twist-bend} \gtrsim \eta_{splay} \gg \eta_{bend}$ (where again $\eta_{twist-bend}$ is dominated by twist). Each of the elasticities and viscosities increase systematically with decreasing temperature, as expected.

Combining our data for the monomer and higher n-mers allows us to compare the magnitudes of the nematic elastic constants over the $n = 1 - 4$ homologous series and, in particular, to compare the measured values to certain predictions for the scaling of these parameters with the length of the n-mer. For flexible elongated ("rodlike") oligomers, and accounting only for entropic effects (which is probably more appropriate for lyotropic than for thermotropic systems), the splay constant K_{11} is expected to scale

different materials, we plot the results against a reduced temperature $(T - T_{NTB})/(T_{NI} - T_{NTB})$. As T decreases, the splay constant K_{11} increases through the full nematic range for all three n-mers, and does not exhibit anomalous pretransitional behavior in the vicinity of the N—N_{TB} transition. With decreasing T, the twist constant K_{22} also increases, but additionally shows a significant pretransitional enhancement near T_{NTB}. The temperature dependence of the bend constant K_{33} reveals an interesting difference among the n-mers. With decreasing T below the N—I transition, K_{33} first decreases monotonically in all the n-mers. In the dimer and tetramer, K_{33} reaches a minimum above the N–N_{TB} transition and then begins to increase up to the transition to the N_{TB} phase. By contrast, K_{33} for the trimer levels off at a minimum value close to T_{NTB} and shows no pretransitional increase.

The temperature-dependence of the ratio K_{11}/K_{22} is presented in Fig. 3(d). For the trimer and tetramer, this ratio exceeds 2 over

as $\bar{L}/D$[47], where $\bar{L}$ is the average extended length of the oligomer, and D is its diameter. On the other hand, for flexible rods, the twist constant K_{22} is expected to scale with the persistence length λ_P – or characteristic length over which unit vectors tangent to the rod lose their correlation – as $K_{22} \sim (\lambda_P/D)^{1/3}$[48]. If $\lambda_P \lesssim \bar{L}$, K_{22} should be basically insensitive to increases in length. Finally, the bend constant should increase with $\bar{L}$ until $\bar{L} \simeq \lambda_P$, where it should saturate. However, we cannot apply this prediction to our system, since for $n > 1$, K_{33} is profoundly affected over the full nematic range by developing N_{TB}-type correlations. These play the dominant role in the behavior of K_{33}, and are outside the scope of the arguments used to make the scaling predictions.
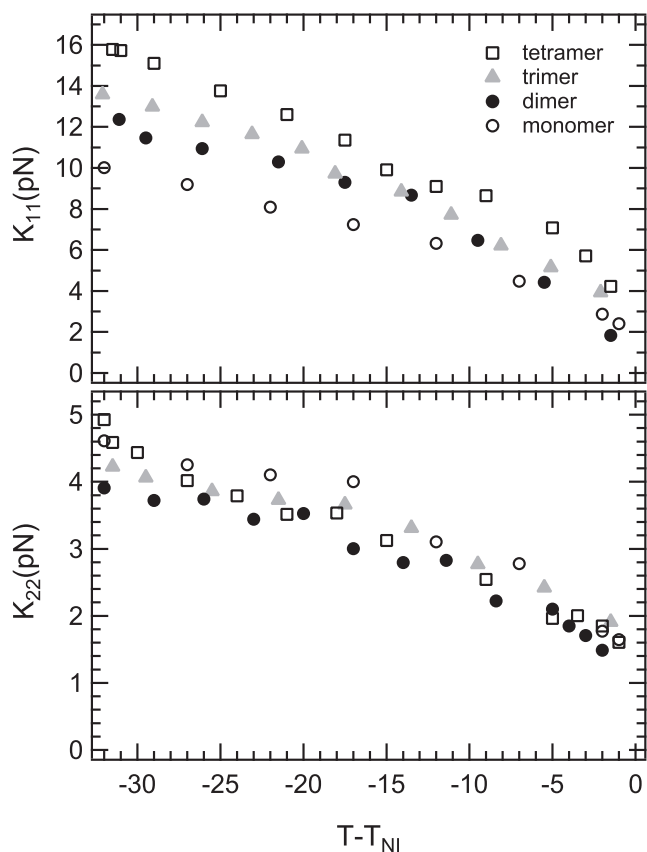
Fig. 6 Splay (K_{11}, top panel) and twist (K_{22}, bottom panel) elastic constants plotted as a function of temperature relative to the nematic-isotropic transition for the studied n-mers.

Fig. 6 plots K_{11} and K_{22} versus $T - T_{NI}$ for $n = 1 - 4$ of the studied n-mer series, down to temperatures just above regime where K_{22} starts increasing due to the developing N_{TB} correlations. The plots provide a direct comparison for different n at the same temperature relative to the N–I transition, as opposed to the plots against the reduced temperature $(T - T_{NTB})/(T_{NI} - T_{NTB})$ in Fig. 3. (The latter is more useful for contrasting the N–N_{TB} pretransitional behavior of the K_{ii} for different n, but is not appropriate for comparing magnitudes at similar $T - T_{NI}$.)

We observe that away from the N–I transition, when the nematic order is well established, the values of K_{22} do not vary systematically with n. This result is consistent with the flexible rod

model, provided λ_P in our flexible n-mers is comparable to the length of a single rigid core unit.

By contrast, for values of $T - T_{NI}$ well into the nematic phase, K_{11} shows a systematic increase with n, though the increase is weaker than one would expect if $\bar{L} \propto n$ and $K_{11}(n)/K_{11}(n = 1) \simeq n$. For example, in the middle of the nematic range in Fig. 6 ($T - T_{NI} = -17°C$), $K_{11}(n = 4)/K_{11}(n = 1) = 1.54$ and $K_{11}(n = 2)/K_{11}(n = 1) = 1.27$. A similar result, $K_{11}(n = 2)/K_{11}(n = 1) = 1.20$ at $T - T_{NI} = -5°C$, was reported by DiLisi et al[49] for a different thermotropic monomer-dimer system. They proposed an explanation for the weaker than expected scaling with n based on including end-end molecular interactions between n-mers, and the excluded volume associated with the molecular ends, in addition to the entropy of mixing "top" and "bottom" ends on which the scaling $K_{11} \propto \bar{L} \propto n$ is predicated. The model including non-entropic interactions qualitatively accounts for weaker dependence of K_{11} on n between thermotropic monomers and dimers, which our results suggest extends up to $n = 4$. In fact, results reported on a 24-mer, where $K_{11}(n = 24)/K_{11}(n = 1) \simeq 10^{50}$, indicate the simple scaling relation may not be accurate even for fairly long thermotopic oligomers. Finally, we should add that in n-mers composed of alternating rigid and flexible elements, the conformational relation between these elements may possibly depend on n, so that the overall length $\bar{L}$ would not necessarily increase linearly with n.

Before proceeding to discuss our main results for the pretransitional behavior of the viscoelastic parameters in terms of the "pseudo-layered" N_{TB} structure, it is important to confirm that mass density correlations (true smectic order) play no significant role in the observed behavior. To that end, we performed small angle X-ray scattering (SAXS) measurements on the n-mers in the N phase and through the N–N_{TB} transition. The measurements were done on the CMS beamline (11-BM) at the National Synchrotron Light Source (NSLS II, Brookhaven National Lab). For the dimer, an aximuthal average of the diffracted intensity reveals two diffuse small angle peaks at scattering wavenumbers corresponding to approximately the length of the dimer ("dimer-like" peak) and to approximately half that length ("monomer"-like peak). As has been found in other N_{TB}-forming dimers, the "monomer"-like peak is more intense.

In Fig. 7, we present the inverse full width at half maximum (FWHM^{-1}) of both "monomer"- and "dimer"-like peaks for the dimer sample as a function of reduced temperature. If the FWHM^{-1} is interpreted as a mass density correlation length, it is clearly limited to length scales on the order of a single monomer throughout the nematic range and well into the N_{TB} phase. Thus, mass density correlations remain extremely short-range over this temperature range.

SAXS data for the higher n-mers reveal additional diffuse peaks at smaller q[51], but the strongest scattering is still associated with the "monomer"-like peak, and the FWHM^{-1} of this peak (see Fig. 7), again confirms short-range density correlations persisting well into the N_{TB} phase of the trimer and tetramer.
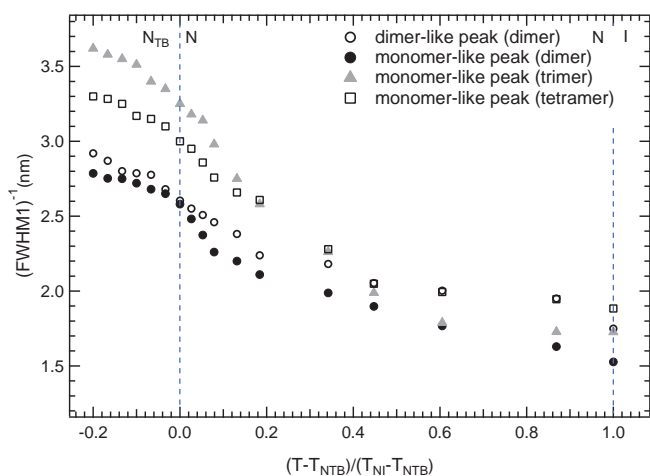
Fig. 7 Inverse full width at half maximum of the "monomer"-like peak, recorded by small-angle X-ray scattering (SAXS) from the studied n-mers, and of the "dimer"-like peak, recorded on the dimer. Data are plotted for reduced temperatures through the N and into the N_{TB} phase. Here "monomer"- and "dimer"-like refer to diffuse peak positions corresponding to approximately the length of the monomer unit and to approximately twice this length. The values of $(FWHM)^{-1}$ were obtained from fitting the azimuthally averaged SAXS profiles to a sum of Lorentzians.

4   Discussion

As mentioned in the previous section, the POM study reveals a well-defined propagating interface at the N—N_{TB} transition, indicating that the transition is first order in the studied n-mers. However, the significant pretransitional behavior of the elastic constants K_{22} and K_{33}, and of the corresponding orientational viscosities (particularly η_{bend}), together with the DSC data (see ESI), suggest that it is weakly first order.

In the following discussion, we will compare the pretransitional behavior of the orientational viscoelastic parameters to the predictions of a coarse-grained model of the N to "pseudo-layered" N_{TB} phase transition. A coarse-grained theory is appropriate for analyzing experimental results when the experiment probes length scales significantly greater than the N_{TB} pitch p_0 – a condition that certainly holds for DLS, since the optical wavelength is ~ 50 times larger than p_0.

Let us therefore consider the impact of fluctuating "pseudo-layered" N_{TB} domains close to the transition. Dozov and Meyer [17,18] have recently explored a symmetry-based analogy between the N_{TB} and chiral smectic-A (SmA*) phases and between the N--N_{TB} and N—SmA* phase transitions. In place of the usual smectic order parameter $\Psi = \psi \exp(iq_0 u)$, where ψ is the amplitude of the smectic density wave and u is the local layer displacement from equilibrium, they define a pseudo-layer order parameter for the N_{TB} phase as $\sigma = \sin\beta \exp(i\delta\phi)$, where β is the tilt angle of the local director $\hat{n}$ away from the average heliconical axis $\hat{z}$, and $\delta\phi$ is the deviation of the phase of $\hat{n}$ from its equilibrium value. The pseudo-layer spacing is the helical pitch, $p_0 = 2\pi/q_0$.

A coarse-grained Landau–de Gennes expansion of the free energy density for the N–N_{TB} transition can then be written down in terms of the pseudo-layer order parameter and coarse-grained nematic director, in direct analogy to the conventional expansion

for the N–SmA* transition (see Eq. S1 in the ESI). As Dozov and Meyer describe, the Landau coefficients and elastic constants appearing in the coarse-grained free energy density should be determined from averaging, over single pitch, a "local" model for the free energy of the N—N_{TB} transition — a model that describes how the heliconical structure develops. One such model, proposed by Dozov [2], is the "elastic instability" model. In this model, the energy of a uniaxial nematic is extended to include fourth order gradients in the director field, thus permitting one or more of the second-order elastic coefficients to become negative and thereby favor a non-uniform local director field. Specifically, the bend elastic constant K_{33} is assumed to be temperature-dependent, $K_{33} = k_{33}^0(T - T^*)$, where k_{33}^0 is a material constant. When T decreases below T^*, K_{33} becomes negative, destabilizing the N phase against bend distortion of the director. To accommodate this bend without defects, the system may transition to either a twist-bend or splay-bend phase. The positive fourth-order elastic terms stabilize the structure for a finite amplitude of the bend distortion. If the "bare" second-order nematic twist and splay constants are related by $K_{11} > 2K_{22}$, as we found in the studied n-mers, the twist-bend phase is favored. In that case, the fourth-order elasticity reduces [2] to a single effective elastic constant C.

Dozov and Meyer have presented the details of averaging the free energy in the "elastic instability" model, and connecting its coefficients to the coarse-grained model, on the N_{TB} side of the transition. To compare with our experimental results, we need to need to follow their approach for the high temperature side (N phase). We outline the procedure in the ESI. Once the relations between coefficients in the two models are determined, one can address the question of the pretransitional behavior of orientational elasticities and viscosities using standard results for the N—SmA transition and employing the specific relations between coefficients.

According to de Gennes' original analysis [52,53] of the N–SmA transition, the pretransitional enhancements of the elastic constants arising from pretransitional fluctuations are given by

$$\delta K_{22} \propto \frac{\xi_\perp^2}{\xi_\parallel}, \ \delta K_{33} \propto \xi_\parallel, \ \delta K_{11} = 0 \tag{1}$$

where $\xi_\perp, \xi_\parallel$ are temperature-dependent correlation lengths specifying the typical size of a fluctuating smectic domain. No pretransitional enhancement is expected for the splay constant; K_{11} should only exhibit a gradual increase due to its dependence on the nematic order parameter, $K_{11} \sim S^2$. However, K_{22} and K_{33} are expected to increase sharply due to the growth of the correlation lengths. Within mean-field theory and after employing the mapping of Landau coefficients between the local and coarse-grained models of the N—N_{TB} transition, we obtain (see ESI) the following expressions for the correlation lengths, which apply to

pseudo-layered N_{TB} domains above the transition:

$$\xi_\perp = \sqrt{\frac{K_{11} + K_{22}}{2(K_{33} + Cq_0^2)}\frac{1}{q_0}}$$

$$\xi_\parallel = \frac{1}{q_0} \tag{2}$$

In these expressions, we assume q_0 (and therefore the pseudo-layer spacing $p_0 = 2\pi/q_0$) could be temperature-dependent on the high temperature side of the transition (i.e., within pretransitional pseudo-layer domains). Then, as described in the ESI, the second expression for $\xi_\perp$ is obtained after expanding $q_0^2(T)$ around the transition temperature T_{NTB} and keeping terms to linear order in $T - T_{NTB}$; it is therefore accurate close to T_{NTB}. The quantity $q_0^{2\prime}(T_{NTB})$ is the first derivative of q_0^2 evaluated at T_{NTB}, and the transition temperature is given by $T_{NTB} = T^* - Cq_0^2(T_{NTB})/k_{33}^0$.

An alternative "local" model of the N_{TB} phase – the "polarization wave" model[15] – invokes a dimensionless helical polarization field $\vec{P}$ (perpendicular to the heliconical axis $\hat{z}$ and with wavenumber q_0) as the N_{TB} order parameter. $\vec{P}$ could represent a shape or form polarization, or a normalized electric polarization, associated with the average conformation of an n-mer molecule. The Landau–de Gennes free energy for this local model is the sum of a standard Landau expansion of $|\vec{P}|$ to fourth order, a gradient term in $\vec{P}$ with effective elastic constant κ, a bilinear coupling between $\vec{P}$ and bend distortions of the director field $\hat{n}$ with coupling coefficient $-\lambda$, and the standard second order Frank elastic energy for distortions in $\hat{n}$. In the ESI, we point out how the polarization wave model produces results for the correlation lengths close to the transition that have the same T and q_0 dependence as in Eq. (2).

We now compare the predictions of Eqs. (1) and (2) to our experimental results for the K_{ii} in the studied n-mers. Strictly speaking, the theoretical results apply to a second order transition, while our optical observations of a propagating front indicate a first order transition. Thus we may expect the predicted pretransitional behavior of the K_{ii} to be cut off at the actual transition temperature T_{NTB}.

Let us first note that in agreement with the prediction of the coarse-grained model, the data for the splay constant K_{11} in Fig. 3(a) show no notable pretransitional behavior as $T \to T_{NTB}$. Second, we observe that Eqs. (1) and (2) imply

$$\frac{\delta K_{22}}{\delta K_{33}} \propto \left(\frac{\xi_\perp}{\xi_\parallel}\right)^2 \propto \frac{1}{T - T_{NTB}},$$

which indicates that K_{22} should exhibit a stronger pretransitional increase than K_{33}. The data for the trimer and tetramer in Fig. 3(b) and 3(c) are consistent with this prediction, although the observable increases in K_{22} are limited due to the first-order nature of the transition. In the dimer, where both K_{22} and K_{33} increase sharply close to T_{NTB}, we note that in cooling the slope of K_{22} vs T starts increasing at a significantly higher temperature than the slope of K_{33}. This is consistent with a stronger temperature dependence of δK_{22}.

A third, and perhaps most illuminating, point of comparison centers on the prediction $\delta K_{33} \propto \xi_\parallel = 1/q_0(T)$ and the different pretransitional behaviors observed for the bend constant among the n-mers. Note again that we allow for the possibility of a temperature-dependent q_0 associated with the fluctuating N_{TB} domains above the transition. In the dimer, K_{33} decreases on cooling through the bulk of the N phase (Fig. 3(a)), as expected from both "local" models of the N—N_{TB} transition. It then turns sharply upward near T_{NTB}. Based on the prediction $\delta K_{33} \propto 1/q_0(T)$, this suggests a significant pretransitional decrease in q_0 as $T \to T_{NTB}$ from above. Carbon-edge[23] and selenium-edge[24] RXS experiments on dimers – the latter on compounds closely related to DTC5C9 – show that q_0 also decreases as $T \to T_{NTB}$ from below the transition. The combination of results suggests that in N_{TB}-forming dimers, q_0 has significant T-dependence on both sides of the transition.

By contrast, our data for K_{33} (Fig. 3(c)) in the homologous trimer reveal no pretransitional enhancement, which would be consistent with $q_0 \approx const$ in the expression for δK_{33} and a fixed (or weakly temperature-dependent) q_0 in the fluctuating N_{TB} domains above T_{NTB}. In addition, the pretransitional increase of K_{22} is weaker in the trimer compared to the dimer (Fig. 3(b)), as expected according to Eqs. (1) and (2) whereby δK_{22} is also proportional to $1/q_0$. Interestingly, recent carbon-edge RXS results on a different trimer[36] demonstrate that $q_0 \approx const$ in the N_{TB} phase as well. Thus, in N_{TB}-forming trimers, q_0 might be a weakly temperature-dependent material parameter.

Finally, our measurements of K_{33} in the tetramer (Fig. 3(c)) are consistent with a T-dependent q_0 that decreases in the N phase as $T \to T_{NTB}$ (though evidently more weakly than in the dimer). Correspondingly, new carbon-edge RXS data on tetramers demonstrate a temperature-dependent, decreasing q_0 as the transition is approached on the N_{TB} side[54]. We can now speculate that the "odd-even" effect observed in the pretransitional behavior of K_{22} and K_{33} is fundamentally connected to the temperature dependence (or lack thereof) of the wavenumber q_0 characterizing the heliconical modulation.

We now turn to the pretransitional behavior of the orientational viscosities in Fig. 4. All of the measured viscosities increase with decreasing temperature through the bulk of the N phase, as expected for an activated (Arrhenius) temperature dependence. Close to T_{NTB}, however, their behavior exhibits clear differences, which we can compare to expectations from the coarse-grained theory of the transition.

For a conventional nematic–smectic-A transition, the singular contributions to these viscosities have been calculated as[55] $\delta\eta_{bend} = \delta\eta_{twist} = \delta\gamma_1$ and $\delta\eta_{splay} = 0$, where γ_1 is the viscosity for pure rotation of the uniaxial nematic director. In the mean field approximation[55,56], $\delta\gamma_1 \propto 1/(a\xi_\parallel)$, where a is the leading Landau coefficient in the conventional free energy density for the N—SmA transition. Then (see ESI) we find $\delta\gamma_1 \propto 1/[(T - T_{NTB})q_0]$ in the case of the "elastic instability" model close to the transition. (A similar result applies for the "polarization wave" model close to the transition.)

The data in Fig. 4 for η_{splay} show no definite evidence of a singular contribution close to the transition, in agreement with the

prediction $\delta\eta_{splay} = 0$. On the other hand, η_{bend} is expected to diverge as $T \to T_{NTB}$, which is consistent with the definite pretransitional enhancement that we observe for this viscosity. Moreover, unlike the case of the bend elastic constant K_{33}, $\delta\eta_{bend}$ is still expected to diverge *even if* q_0 is temperature-independent. Thus, for the trimer, the absence of a pretransitional effect on K_{33} (attributed to fixed q_0) and the presence of one in η_{bend} are fully consistent with the coarse-grain theory and, in particular, with the N_{TB}/SmA* analogy on which it is based.

Our data for the viscosity $\eta_{twist-bend}$, which is dominated by twist, show much weaker evidence of pretransitional enhancement than η_{bend}. Although this appears to be inconsistent with the prediction above, it may simply be that over the accessible pretransitional range, the enhancement of the twist viscosity is small compared to the non-singular part of $\eta_{twist-bend}$, which is nearly 10 times larger than the non-singular component of η_{bend}. A more accurate measurement of pure twist fluctuations would be helpful to clarify the issue.

5 Conclusions

We prepared novel LC trimer and tetramer homologues, and measured the orientational elastic constants and associated viscosities of these materials, together with the homologous dimer, throughout the nematic range including the pretransitional region above the nematic to twist-bend nematic phase transition. The ratio of splay to twist elastic constants exceeds 2 in the majority of the nematic range for all three oligomers; this satisfies the theoretical criterion for a uniaxial to twist-bend nematic transition at lower temperature. The bend and twist elastic constants show sharp enhancements close to the N—N_{TB} transition in even n-mers (dimer and tetramer), while in the odd n-mer (trimer) the bend constant shows no pretransitional increase. The splay constant shows no notable enhancement in any n-mer. Among the orientational viscosities, the bend viscosity exhibits strong pretransitional enhancement in the even n-mers and a somewhat weaker enhancement in the odd n-mer.

We discussed the pretransitional behavior of the viscoelastic parameters in terms of a coarse-graining of two proposed "local" models of the N_{TB} phase, which results in a free energy density analogous that for the nematic to smectic-A transition. The analysis of our experimental results in this framework suggests that the wavenumber characterizing heliconical fluctuations in the N phase depends significantly on temperature in the dimer and tetramer as the N–N_{TB} transition is approached, but remains essentially constant in the trimer.

Our results raise intriguing theoretical and experimental challenges for future investigation. On the theoretical side, the "local" and coarse-grained models need to be extended to treat a first order N—N_{TB} transition. In the coarse-grained free energy, one can add a (positive) sixth order term in the order parameter describing the N_{TB} "pseudo-layers". This would produce a first-order phase transition if the coefficient of the fourth order term is negative and a tricritical point if it vanishes. De Gennes described how this could happen for the N—SmA transition due to coupling between nematic and smectic order parameters[46]; a parallel mechanism might apply to a nematic to "pseudo-layer" transition with

similar symmetry. In terms of the "local" models, one can straightforwardly extend the "polarization wave" theory by adding a sixth order term to the Landau expansion of the polarization field and admitting the possibility of a negative coefficient for the fourth order term.

A second major challenge for theory is understanding the selection of the characteristic wavenumber of the heliconical modulation in pretransitional, fluctuating N_{TB} domains, and its temperature dependence as the transition is approached. There are ongoing efforts, based on the "polarization" wave model, to address these questions[57].

Experimentally, it is important to investigate at the temperature dependence of the viscoelastic parameters in additional n-mer systems – e.g., homologues of the n-mers studied in the present work with odd-membered linkers of different length, or mixtures of odd and even n-mers – that might exhibit larger pretransitional enhancements of K_{22} and K_{33}, as the N_{TB} phase is approached from above. That could allow a more quantitative comparison of experimental results to the relevant predictions of the coarse-grained models.

Conflicts of interest

There are no conflicts to declare.

Acknowledgements

Notes and references

1 R. B. Meyer, *Les houches summer school in theoretical physics XXV-1973*, Gordon and Breach, New York, 1976, pp. 273–373.

2 I. Dozov, *Europhys. Lett.*, 2001, **56**, 247–253.

3 V. L. Lorman and B. Mettout, *Physical Review Letters*, 1999, **82**, 940–943.

4 T. C. Lubensky and L. Radzihovsky, *Physical Review E - Statistical Physics, Plasmas, Fluids, and Related Interdisciplinary Topics*, 2002, **66**, year.

5 R. Memmer, *Liquid Crystals*, 2002, **29**, 483–496.

6 M. Cestari, S. Diez-Berart, D. A. Dunmur, A. Ferrarini, M. R. De La Fuente, D. J. B. Jackson, D. O. Lopez, G. R. Luckhurst, M. A. Perez-Jubindo, R. M. Richardson, J. Salud, B. A. Timimi and H. Zimmermann, *Physical Review E*, 2011, **84**, 031704.

7 V. Borshch, Y. K. Kim, J. Xiang, M. Gao, A. Jákli, V. P. Panov,

J. K. Vij, C. T. Imrie, M. G. Tamba, G. H. Mehl and O. D. Lavrentovich, *Nature Communications*, 2013, **4**, 2635–1–8.

8 D. Chen, J. H. Porada, J. B. Hooper, A. Klittnick, Y. Shen, M. R. Tuchband, E. Korblova, D. Bedrov, D. M. Walba, M. A. Glaser, J. E. Maclennan and N. A. Clark, *Proceedings of the National Academy of Sciences*, 2013, **110**, 15931–15936.

9 C. Meyer, G. R. Luckhurst and I. Dozov, *Physical Review Letters*, 2013, **111**, 1–5.

10 E. Gorecka, M. Salamonczyk, A. Zep, D. Pociecha, C. Welch, Z. Ahmed and G. H. Mehl, *Liquid Crystals*, 2015, **42**, 1–7.

11 V. Panov, M. Nagaraj, J. Vij, Y. Panarin, A. Kohlmeier, M. Tamba, R. Lewis and G. Mehl, *Physical Review Letters*, 2010, **105**, 167801.

12 P. A. Henderson and C. T. Imrie, *Liquid Crystals*, 2011, **38**, 1407–1414.

13 K. Adlem, M. Čopič, G. R. Luckhurst, a. Mertelj, O. Parri, R. M. Richardson, B. D. Snow, B. a. Timimi, R. P. Tuffin and D. Wilkes, *Physical Review E*, 2013, **88**, 022503.

14 V. Görtz, C. Southern, N. W. Roberts, H. F. Gleeson and J. W. Goodby, *Soft Matter*, 2009, **5**, 463–471.

15 S. M. Shamid, S. Dhakal and J. V. Selinger, *Physical Review E*, 2013, **87**, 052503.

16 E. I. Kats and V. V. Lebedev, *JETP Letters*, 2014, **100**, 110–113.

17 C. Meyer and I. Dozov, *Soft Matter*, 2016, **12**, 574–580.

18 I. Dozov and C. Meyer, *Liquid Crystals*, 2017, **44**, 4–23.

19 M. Kleman and K. S. Krishnamurthy, *Physical Review E*, 2018, **98**, 032705.

20 V. P. Panov, R. Balachandran, M. Nagaraj, J. K. Vij, M. G. Tamba, a. Kohlmeier and G. H. Mehl, *Applied Physics Letters*, 2011, **99**, 261903.

21 L. Beguin, J. W. Emsley, M. Lelli, A. Lesage, G. R. Luckhurst, B. A. Timimi and H. Zimmermann, *Journal of Physical Chemistry B*, 2012, **116**, 7940–51.

22 J. Carvalho, C. Cruz, J. L. Figueirinhas, M. G. Tamba, A. Kohlmeier and G. H. Mehl, *Journal of Physical Chemistry B*, 2019, DOI:10.1021/acs.jpcb.8b11526.

23 C. Zhu, M. R. Tuchband, A. Young, M. Shuai, A. Scarbrough, D. M. Walba, J. E. Maclennan, C. Wang, A. Hexemer and N. A. Clark, *Physical Review Letters*, 2016, **116**, 147803.

24 W. D. Stevenson, Z. Ahmed, X. B. Zeng, C. Welch, G. Ungar and G. H. Mehl, *Physical Chemistry Chemical Physics*, 2017, **19**, 13449–13454.

25 M. Salamończyk, N. Vaupotič, D. Pociecha, C. Wang, C. Zhu and E. Gorecka, *Soft Matter*, 2017, **13**, 6694–6699.

26 M. Salamończyk, R. J. Mandle, A. M. Makal, A. Liebman-Peláez, J. Feng, J. W. Goodby and C. Zhu, *Soft Matter*, 2018.

27 Z. Parsouzi, S. M. Shamid, V. Borshch, P. K. Challa, M. G. Tamba, C. Welch, G. H. Mehl, J. T. Gleeson, A. Jakli, O. D. Lavrentovich, D. W. Allender, J. V. Selinger and S. Sprunt, *Physical Review X*, 2016, **6**, 021041.

28 Z. Parsouzi, S. A. Pardaev, C. Welch, Z. Ahmed, G. H. Mehl, A. R. Baldwin, J. T. Gleeson, O. D. Lavrentovich, D. W. Allender, J. V. Selinger, A. Jakli and S. Sprunt, *Phys. Chem. Chem. Phys.*, 2016, **18**, 31645–31652.

29 C. J. Yun, M. R. Vengatesan, J. K. Vij and J. K. Song, *Applied Physics Letters*, 2015, **106**, year.

30 S. A. Pardaev, S. M. Shamid, M. G. Tamba, G. H. Mehl, J. T. Gleeson, D. W. Allender, J. V. Selinger, B. Ellman, A. Jakli and S. Sprunt, *Soft Matter*, 2016, **12**, 1–11.

31 R. J. Mandle, *Soft Matter*, 2016, **12**, 7883–7901.

32 R. J. Mandle and J. W. Goodby, *RSC Advances*, 2016, **6**, 34885–34893.

33 R. J. Mandle, M. P. Stevens and J. W. Goodby, *Liquid Crystals*, 2017, **44**, 2046–2059.

34 F. P. Simpson, R. J. Mandle, J. N. Moore and J. W. Goodby, *Journal of Materials Chemistry C*, 2017, **5**, 5102–5110.

35 Y. Wang, G. Singh, D. M. Agra-Kooijman, M. Gao, H. Krishna Bisoyi, C. Xue, M. R. Fisch, S. Kumar and Q. Li, *CrystEngComm*, 2015, **17**, 2778–2782.

36 M. R. Tuchband, D. A. Paterson, M. Salamonczyk, V. A. Norman, A. Scarbrough, E. Garcia, C. Wang, J. M. D. Storey, D. M. Walba, S. N. Sprunt, A. Jakli, C. Zhu, C. T. Imrie and N. A. Clark, *arXiv:1710.00922 [cond-mat.soft]*, 2017.

37 R. J. Mandle and J. W. Goodby, *Chemphyschem*, 2016, **17**, 967–970.

38 W. D. Stevenson, H.-X. Zou, X.-B. Zeng, C. Welch, G. Ungar and G. H. Mehl, *Physical Chemistry Chemical Physics*, 2018, **20**, 25268–25274.

39 M. Bradshaw and P. Raynes, *J. Phys. France*, 1985, **46**, 1513–1520.

40 N. V. Madhusudana and R. Pratibha, *Molecular Crystals and Liquid Crystals*, 1982, **89**, 249–257.

41 B. Kundu, R. Pratibha and N. V. Madhusudana, *Physical Review Letters*, 2007, **99**, 247802.

42 G. Babakhanova, Z. Parsouzi, S. Paladugu, H. Wang, Y. A. Nastishin, S. V. Shiyanovskii, S. Sprunt and O. D. Lavrentovich, *Physical Review E*, 2017, **96**, 062704.

43 D. Sharma, J. C. MacDonald and G. S. Iannacchione, *J. Phys. Chem. B*, 2006, **110**, 16679–16684.

44 B. R. Ratna and S. Chandrasekhar, *Mol. Cryst. Liq. Cryst.*, 1988, **162**, 157–159.

45 M. A. Anisimov, P. E. Cladis, E. E. Gorodetskii, D. A. Huse, V. E. Podneks, V. G. Taratuta, W. Van Saarloos and V. P. Voronov, *Physical Review A*, 1990, **41**, 6749–6762.

46 P. G. de Gennes and J. Prost, *The Physics of Liquid Crystals*, Clarendon Press, Oxford, UK, 2nd edn, 1993.

47 V. G. Taratuta, F. Lonberg and R. B. Meyer, *Phys. Rev. A*, 1988, **37**, 1831R–1834R.

48 T. Odijk, *Liquid Crystals*, 1986, **1**, 553–559.

49 G. A. DiLisi, C. Rosenblatt, A. C. Griffin and U. Hari, *Liquid Crystals*, 1990, **8**, 437–443.

50 S. Zheng-Min and M. Kleman, *Mol. Cryst. Liq. Cryst.*, 1984, **111**, 321–328.

51 R. Saha et al, *submitted to Materials Horizons*.

52 P. G. de Gennes, *Solid State Communications*, 1993, **88**, 1039–1042.

53 P. G. de Gennes, *Mol Cryst Liq Cryst*, 1973, **21**, 49–76.

54 M. Salamończyk, *unpublished*.

55 F. Jähnig and F. Brochard, *Journal de Physique*, 1974, **35**, 301–313.

56 D. Langevin, *J. Phys. France*, 1976, **37**, 901.

57 A. Jakli, O. D. Lavrentovich and J. V. Selinger, *Reviews of Modern Physics*, 2018, **90**, 045004.